PNAS Tracking # 2015-00925R

Potent organo-osmium compound shifts metabolism in epithelial ovarian cancer cells

Jessica M. Hearn, Isolda Romero-Canelón, Alison F. Munro, Ying Fu, Ana M. Pizarro, Mathew J. Garnett, Ultan McDermott, Neil O. Carragher and Peter J. Sadler*

Supporting Information

Materials. For the biological experiments, RPMI-1640 medium, as well as foetal bovine serum, L-glutamine, penicillin/streptomycin mixture, trypsin, trypsin/EDTA, phosphate buffered saline (PBS) were purchased from PAA Laboratories GmbH. HPLC grade ethanol, β-mercaptoethanol, PI (>94%) and RNAse A were obtained from Sigma Aldrich together with the Annexin V-FITC Apoptosis Detection Kit. The ROS determination kit was obtained from Enzo Life Sciences. For RNA sequencing, Qubit reagents were obtained from Life Technologies and QIAShredder and RNeasy plus mini kit from Qiagen. Compounds **1-4** were isolated and used as their PF_6 salts, synthesized and characterized as described previously, **1** ([Os(η^6-*p*-cymene)(4-(2-pyridylazo)-N,N-dimethylaniline)I]PF_6) (1,2), **2** ([Os(η^6-*p*-cymene)(2-pyridylazoaniline)Cl]PF_6) (1), **3** ([Os(η^6-biphenyl)(4-(2-pyridylazo)-chloroaniline)Cl]PF_6) (2), and **4** ([Os(η^6-*p*-cymene)((4-(2-pyridinylmethylene)amino)phenol)I]PF_6) (3).

Cell maintenance. A2780 ovarian cancer cells were obtained from ECACC (European Collection of Animal Cell Culture) together with A549, HCT116, MCF7 and PC3 cells of lung, colon, breast and prostate origin, respectively. A2780 and PC3 cells were grown as single monolayers in RPMI-1640 medium, while DMEM was used for A549 and MCF7 and McCoy 5A for HCT116 cells. In all cases culture medium was supplemented with 10% (v/v) fetal calf serum, 1% (v/v) 2 mM L-glutamine and 1% (v/v) penicillin (10 k units/mL)/streptomycin (10 mg/mL), at 310 K in a humidified atmosphere containing 5% CO_2. Maintenance passages were done at *ca*. 80% confluency.

***In vitro* growth inhibition assay.** Briefly, 96-well plates were used to seed 5000 cells per well; they were left to pre-incubate in drug-free media at 310 K for 48 h before adding various concentrations of the compounds to be tested. Stock solutions of the Os(II) compounds were firstly prepared in 5% DMSO and a mixture 0.9% w/v saline and medium (1:1) following serial dilutions in the corresponding cell culture medium. A drug exposure period of 24 h was allowed. After this, the supernatant were removed by suction and each well was washed with PBS. A further 72 h was allowed for the cells to recover in drug-free medium at 310 K. The SRB assay was used to determine cell viability. This assay, first developed by Skehan et al. in 1990 (4) and further modified by Vichai (5), it is based on the ability of the sulforhodamine B to bind electrostatically to basic amino acid residues of proteins from fixed cells. Absorbance measurements of solubilized dye allow the determination of the amount of viable treated cells against an untreated control. These measurements were carried out using a BioRad iMark microplate reader with a 470 nm filter. IC_{50} values, as the concentration which causes 50% of inhibition

of cell growth, were determined as duplicates of triplicates in two independent sets of experiments, and their standard deviations calculated.

PEO1/PEO4 ovarian cancer cell model. The PEO1/PEO4 ovarian cancer cell model represents a matched pair of cell lines developed within the Edinburgh Cancer Research Centre which have been isolated from a single patient with high grade serous ovarian cancer before (PEO1) and after (PEO4) clinical resistance had developed within the patient following platinum therapy (6).

MTT cell viability assay on PEO1/PEO4 cell model. The MTT 3-(4,5-dimethylthiazol-2-yl)-2,5-diphenyltetrazolium assay was performed as previously described with minor modifications (7). Briefly, 5000 PEO1 or PEO4 cells were plated into each well of a standard 96-well plate and allowed to adhere and proliferate for 48 h in drug-free medium prior to addition of compound **1**. An 8-point half-log dose response to compound **1** was prepared in DMSO at 1000x final assay volume and subsequently diluted and added to cell culture plates. Vehicle control (0.1% v/v DMSO) samples were also present on every plate. After 5 days of compound treatment, 20 μL of 5 mg/mL MTT solution (VWR international) was added to each well and incubated at 37°C for 4 hours. Media/MTT solution was gently aspirated and 50 μL of DMSO added per well and incubated for at least 3 min at room temperature prior to reading absorbance on a standard bench top plate reader with 540 nm filter. Absorbance readings from compound-treated samples were normalized to vehicle control and curve fitting (four-parameter logistic variable slope model) was performed using Graphpad Prism software to obtain EC_{50} values.

RNA sequencing. Cells were seeded at 3×10^6 in P100 Petri dishes and left to incubate for 24 h at 310 K in a humidified atmosphere containing 5% CO_2. Stock solutions of the negative control and compound **1** were prepared in 5% DMSO, 10% saline, and 85% RPMI-1640 medium. Cells were exposed to compound **1** at a final concentration of 150 nM. After 4, 12, 24 and 48 h exposure, medium was removed from triplicate compound-exposed and control-exposed dishes, and cells were washed twice with PBS and collected using trypsin. Between 5×10^6 and 1×10^7 cells in each sample were taken forward for RNA extraction. Using QIAshredder spin columns (Qiagen), the cells were lysed, as per manufacturer's instructions. DNA was eliminated from each sample using gDNA spin columns, and the RNA was purified using RNeasy spin columns and buffer solutions (RNeasy plus mini kit, QIagen) as per the manufacturer's instructions. RNA was collected in 70 µL RNase-free water and stored at 193 K.

All samples were quality controlled-checked using a NanoDrop 1000 spectrophotometer, to estimate RNA concentration and to determine the presence of salt/protein impurities. All samples had $A_{260}/A_{280} \geq 2.0$ and $A_{260}/A_{230} \geq 1.9$. The RNA was verified using a 2100 Agilent Bioanalyzer and an RNA 6000 Nano Kit (Agilent), and the Qubit assay (Life Technologies). All samples had RIN = 10. Samples were then shipped on dry ice to the Oxford Genomics Centre for Truseq RNA library preparation (Illumina) and 50bp paired-end sequencing on an Illumina HiSeq2000 machine with approximately 30 million paired-end reads per sample (Tables S1 and S2). Sequence reads were mapped to the hg19 (GRCh37) genome using Tophat2 (Table S2). Differential expression was calculated using HTSeq and edgeR software.

RPPA. 4 x 10^5 cells were seeded per well in 6-well plates, with samples in duplicate. Cells were pre-incubated in drug-free media for 48 h in a 5% CO_2 humidified atmosphere. After this, cells were treated with compound **1** at 150 nM and 450 nM for 4, 24, 48 and 72 h. Control samples were treated with medium containing 0.1% v/v DMSO. Following exposure, the drug-containing medium was removed, and cells were washed x2 with PBS and lysed with CLB1 buffer (Zepotsens, Bayer) according to manufacturer's instructions.

Cell lysates were normalized to a uniform protein concentration of 2 mg/mL with spotting buffer CSBL1 (Zeptosens-Bayer) prior to preparing a final 4-fold concentration series of 0.2, 0.15, 0.1, and 0.75 mg/mL. The diluted concentration series for each sample was printed onto hydrophobic Zeptosens protein microarray chips (ZeptoChip™, Zeptosens-Bayer) under environmentally controlled conditions (constant 50% humidity and 14 ºC temperature) using a non-contact printer (Nanoplotter 2.1e, GeSiM). A single 400 pL droplet of each lysate concentration was deposited onto the Zeptosens chip. A reference grid of AlexaFluor647 conjugate BSA consisting of 4 column X 22 rows was spotted onto each sub-array, each sample concentration series was spotted in between reference columns. After array printing, the arrays were blocked with an aerosol of BSA solution using a custom-designed nebulizer device (ZeptoFOG™, Zeptosen-Bayer) for 1 h to prevent non-specific antibody binding. The protein array chips were subsequently washed in double-distilled water and dried prior to performing a dual antibody immunoassay comprising of a 24 h incubation with primary antibodies (Table S3) followed by 2.5 h incubation with secondary Alexa-Fluor A647 conjugated antibody detection reagent (anti-rabbit or anti-mouse A647 Fab, Invitrogen).

Following secondary antibody incubation and a final wash step in BSA solution, the immunostained arrays were imaged using the ZeptoREADER™ instrument (Zeptosens-Bayer). For each sub-array, five separate images were acquired using different exposure times ranging from 0.5-10 s. Microarray images representing the longest exposure without saturation of fluorescent signal detection were automatically selected for analysis using the ZeptoView™ 3.1 software. A weighted linear fit through the 4-fold concentration series was used to calculate the relative fluorescence intensity (RFI) value for each sample replicate. Local normalization of sample signal to the reference BSA grid was used to compensate for any intra- or inter-array/chip variation. Local normalized RFI values were subsequently normalized to the appropriate DMSO vehicle control samples to represent the relative abundance of total, phosphorylated and cleaved proteins in compound-treated sample relative to DMSO control for each time point.

ROS Determination. Flow cytometry analysis of ROS/superoxide generation in A2780 cells induced by exposure to compound **1**, was carried out using the Total ROS/Superoxide detection kit (Enzo Life Sciences) according to the supplier's instructions. This kit included two fluorescent staining reagents: the first responds to total oxidative stress levels (the combined levels of peroxides, peroxynitrites and hydroxyl radicals, etc.; green), and the second reagent specifically detects superoxide (orange). Briefly, 1.5×10^6 A2780 cells per well were seeded in a 6-well plate. Cells were pre-incubated in drug-free media at 310 K for 24 h in a 5% CO_2 humidified atmosphere, then compound **1** was added at 150 nM. After 24 h of drug exposure, supernatants were removed by suction and cells were washed with PBS. Finally, cells were harvested using

trypsin. Staining was achieved by re-suspending the cell pellets in buffer containing the orange/green fluorescent reagents. Cells were analysed in a Becton Dickinson FACScan Flow Cytometer using Ex/Em: 490/525 nm for oxidative stress and Ex/Em: 550/620 nm for superoxide detection. Data were processed using Flowjo software.

Following the procedure described, we also measured the production of ROS and superoxide in A2780 cells exposed to 3 other Os(II) compounds structurally closely related to compound **1** ([Os(η^6-*p*-cym)(NMe_2-azpy)I]PF_6; IC_{50}=0.15 ± 0.01 μM), namely compound **2** ([Os(η^6-*p*-cym)(azpy)Cl]PF_6; IC_{50} >100 μM), compound **3** ([Os(η^6-bip)(Cl-azpy)Cl]PF_6; IC_{50} >100 μM) and compound **4** ([Os(η^6-*p*-cym)(OH-impy)I]PF_6; IC_{50}= 30 ± 2 μM) (SI Appendix Table 5 and SI Appendix Fig. 6). Furthermore the ROS and superoxide induction by compound **1** and compound **4** were measured in A549 lung, HCT116 colon, MCF7 breast and PC3 prostate cancer cells following similar procedures (SI Appendix Table S6 and SI Appendix Fig. S7).

Apoptosis. The induction of apoptosis was investigated in A2780 cells using Annexin V FITC and propidium iodide (PI) double staining. Briefly, 2.5 × 10^6 cells were seeded per well in 6-well plates. Cells were pre-incubated in drug-free media at 310 K for 24 h in a 5% CO_2 humidified atmosphere. After this, cells were treated with compound **1** at 150 nM for 24 h. Following exposure, the drug-containing medium was removed, and cells were washed, harvested and stained with Annexin V FITC and propidium iodide (Biovision, Annexin V-FITC Apoptosis Kit) according to the manufacturer's instructions. Control samples stained with just PI or Annexin V FITC were also included for

compensation purposes. The samples were analysed using FACS Calibur flow cytometer running Cell Quest software (20000 events were collected from each sample). Data were processed using Flowjo software (SI Appendix Table S7).

NCI/DTP Cytotoxicity. Compound **1** was evaluated by the National Cancer Institute Developmental Therapeutics Program (NCI/DTP, U.S.A.) for *in vitro* cytotoxicity towards *ca*. 60 human cancer cell lines. The cells were treated with **1** for 48 h at 5 concentrations ranging from 0.01 to 100 μM. The protocol for the determination of cytotoxicity in the 60-cell line panel can be found at http://dtp.nci.nih.gov/branches/btb/ivclsp.html. The DTP homepage can be accessed at http://dtp.cancer.gov/.

Sanger Institute screening. Compound **1** was evaluated by the Sanger Institute as part of the Cancer Genome Project, for *in vitro* activity towards 809 cancer cell lines. The cells were treated with compound **1** for 72 h across a 9-point concentration range. Full protocols details can be found at http://www.cancerrxgene.org/help/, the project home page can be found at https://www.sanger.ac.uk/research/projects/cancergenome/.

Tables

Table S1. Summary of RNAseq lane coverage.

Lane	Yield (Mb Q20)	Clusters	% Mapped reads	% Coverage	Mean quality score
1.1	10992.16	5701716	98.8	3.9	35.7
1.2	10007.96	5701716	97.4	3.9	33.0
2.1	9445.20	4374075	98.1	4.0	36.7
2.2	8846.46	4374075	97.7	4.1	34.4
3.1	9871.37	4625953	98.7	3.8	36.5
3.2	9210.49	4625953	98.2	3.8	34.1
4.1	8292.52	1900942	98.5	3.0	36.8
4.2	8075.68	1900942	98.0	3.0	36.1
5.1	8542.75	1954555	98.5	3.6	36.8
5.2	8318.13	1954555	98.1	3.6	36.0

Table S2. Summary of RNAseq sample coverage and mapping statistics.

Sample Number	Sample Name	Yield (Mb)	Number of reads	% Mapped	% Properly paired	Mean Quality score (PF)
1	0 h control	2907.96	58,435,334	98.53	78.45	36.5
2	0 h control	2630.31	52,952,428	98.32	77.97	36.4
3	0 h control	2615.74	52,411,032	98.11	77.80	36.5
4	0 h compound **1**	2865.17	57,489,392	98.72	77.66	36.5
5	0 h compound **1**	2633.42	53,112,138	97.75	76.37	36.5
6	0 h compound **1**	2729.00	54,962,488	98.12	76.14	36.4
7	4 h control	3909.89	82,071,522	98.19	75.01	34.4
8	4 h control	4026.19	84,555,686	98.11	80.47	34.4
9	4 h control	3491.13	73,333,434	97.93	74.80	34.4
10	4 h compound **1**	3289.76	69,130,568	97.87	76.60	34.4
11	4 h compound **1**	2848.74	59,742,704	97.99	75.40	34.5
12	4 h compound **1**	3154.27	72,018,526	98.38	75.66	34.4
13	12 h control	2885.78	50,690,134	97.87	76.58	36.4
14	12 h control	2781.76	55,041,730	99.25	76.72	36.4
15	12 h control	2514.15	60,723,390	97.88	75.91	36.4
16	12 h compound **1**	2746.99	58,813,794	98.12	76.44	36.4
17	12 h compound **1**	3010.89	57,945,078	98.82	84.52	36.4
18	12 h compound **1**	2921.30	56,092,354	97.97	75.97	36.4
19	24 h control	2949.76	60,331,926	98.14	75.18	35.6
20	24 h control	3330.48	67,939,036	98.93	76.00	35.0
21	24 h control	2895.71	59,240,982	98.09	75.24	35.6
22	24 h compound **1**	3109.75	60,331,926	95.65	73.64	35.5
23	24 h compound **1**	3010.05	67,939,036	98.48	75.83	35.6
24	24 h compound **1**	2995.90	59,240,982	98.18	76.14	35.5
25	48 h control	3362.02	69,027,526	98.61	73.88	35.4
26	48 h control	3181.34	65,550,492	97.69	73.60	35.3
27	48 h control	2684.67	55,141,160	98.55	74.04	35.3
28	48 h compound **1**	3250.36	66,793,080	98.39	74.03	35.4
29	48 h compound **1**	3233.01	66,227,334	99.20	74.44	35.3
30	48 h compound **1**	3370.46	69,306,494	98.19	73.63	35.3

Table S3. Protein modifications detected by antibodies, and antibody catalogue numbers

Exact target	Company	Catalogue Number	Description in manuscript
ATM	Merck (calbiochem)	PC116	ATM
ATM/ATR Substrate P Ser/Thr	Cell Signalling Technol.	2851	ATM*
cdc25A	Cell Signalling Technol.	3652	CDC25A
cdc25c P Ser216	Cell Signalling Technol.	4901	CDC25A*
p21 CIP/WAF1	Cell Signalling Technol.	2946	p21
p21 CIP/WAF1 p Thr145	Santa Cruz	20220-R	p21*
p53	Cell Signalling Technol.	9282	p53
p53 P Ser15	Cell Signalling Technol.	9284	p53*
BAD P Ser112 (BAD*)	Cell Signalling Technol.	9291	Pro-apoptotic
BAD P Ser136 (BAD(*))	Cell Signalling Technol.	9295	Pro-apoptotic
BAK	Epitomics	1542-1	Pro-apoptotic
BAX	Epitomics	1063	Pro-apoptotic
BCL-2	Epitomics	1017-1	Pro-apoptotic
BCL-2 P Ser70 (BCL-2*)	Cell Signalling Technol.	2827	Pro-apoptotic
BID	Epitomics	1008	Pro-apoptotic
Caspase 3 (CASP3)	Cell Signalling Technol.	9662	Pro-apoptotic
Caspase 3 cleaved (CASP3*)	Cell Signalling Technol.	9664	Pro-apoptotic
PARP cleaved Asp214 (PARP*)	Cell Signalling Technol.	9541	Pro-apoptotic
PTEN	Cell Signalling Technol.	9552	Pro-apoptotic
PTEN P Ser380,Thr382,Thr383 (PTEN*)	Cell Signalling Technol.	9554	Pro-apoptotic
PUMA	Cell Signalling Technol.	4976	Pro-apoptotic
BCL-X	Epitomics	1018	Anti-apoptotic
BIM	Epitomics	1036	Anti-apoptotic
PARP	Cell Signalling Technol.	9542	Anti-apoptotic
Survivin	Cell Signalling Technol.	2808	Anti-apoptotic
XIAP	Cell Signalling Technol.	2045	Anti-apoptotic

Table S4. Flow cytometry data for the levels of superoxide and total ROS in A2780 cells exposed to compound **1** at 150 nM for 24 h. The quadrants refer to the percentage of cells in 4 separated sections in the ROS flow cytometry traces shown in Figure 2C. FL1 measures total ROS, where FL1-H- = low measurement and FL1-H+ = high measured levels. FL2 measures superoxide levels, where FL2-H- = low levels measured and FL2-H+ = high levels of superoxide measured. Negative control refers to exposure of cells to drug-free medium, positive controls were exposed to pyocyanin.

Quadrants	% population ± SD		
	Compound **1** (0.15 μM)	-ve control	+ve control
Q1: FL1-H- / FL2-H+	1.65 ± 0.09	0.002 ± 0.003	0.03 ± 0.02
Q2: FL1-H+ / FL2-H+	95.4 ± 0.2	0.00 ± 0.01	99 ± 2
Q3: FL1-H+ / FL2-H-	2.47 ± 0.08	0.00 ± 0.01	0.00 ± 0.01
Q4: FL1-H- / FL2-H-	0.41 ± 0.02	100.00 ± 0.01	0.02 ± 0.01

Table S5. Comparison of flow cytometry data for the levels of superoxide and total ROS in A2780 cells exposed to compounds **1 - 4** for 24 h. FL1 channel measures total ROS and FL2 channel measures superoxide levels. The percentages shown represent the populations with high fluorescence in a given channel determined by the gating of a dot plot according to the controls. Negative controls were obtained using untreated cells and positive controls were A2780 cells exposed to pyocyanin.

Compounds[a]	IC_{50} (μM)	% population ± SD	
		FL1 Channel	FL2 Channel
1	0.15 ± 0.01	97.91 ± 0.08	97.08 ± 0.07
2	> 100	97.9 ± 0.2	10.72 ± 0.08
3	>100	99.43 ± 0.06	32 ± 1
4	30 ± 2	99.1 ± 0.5	92.2 ± 0.4
Negative	-	0.2 ± 0.1	0.3 ± 0.1
Positive	-	99.5 ± 0.2	99.8 ± 0.3

[a] Compounds: **1** ([Os(η^6-*p*-cymene)(4-(2-pyridylazo)-N,N-dimethylaniline)I]PF_6), **2** ([Os(η^6-*p*-cymene)(2-pyridylazoaniline)Cl]PF_6), **3** ([Os(η^6-biphenyl)(4-(2-pyridylazo)-chloroaniline)Cl]PF_6) and **4** ([Os(η^6-*p*-cymene)((4-(2-pyridinyl methylene)amino)phenol)I]PF_6).

Table S6. Flow cytometry data for the levels of superoxide and total ROS in A549 (lung), HCT116 (colon), MCF7 (breast) and PC3 (prostate) cancer cells exposed to compound **1** ([Os(η^6-*p*-cym)(NMe_2-azpy)I]PF_6) or compound **4** ([Os(η^6-*p*-cym)(OH-impy)I]PF_6) for 24 h. FL1 channel measures total ROS and FL2 channel measures superoxide levels. The percentages shown represent the populations with high fluorescence in a given channel determined by the gating of a dot plot according to the controls. Negative controls were obtained using untreated cells and positive controls were A2780 cells exposed to pyocyanin.

Cell line	IC_{50} (μM)		% population ± SD			
	Compound **1**	Compound **4**	Compound **1**		Compound **4**	
			FL1 Channel	FL2 Channel	FL1 Channel	FL2 Channel
A2780	0.15 ± 0.01	30 ± 2	97.9 ± 0.1	97.19 ± 0.07	99.1 ± 0.5	92.2 ± 0.4
A549	0.28 ± 0.03	48 ± 3	100 ± 2	99.6 ± 0.5	82.8 ± 0.6	76.2 ± 0.4
HCT116	0.26 ± 0.03	>100	99.9 ± 0.1	74.4 ± 0.6	99.99 ± 0.06	13.7 ± 0.7
MCF7	0.12 ± 0.02	>100	99.9 ± 0.3	62.7 ± 0.9	99.92 ± 0.03	12.6 ± 0.5
PC3	0.65 ± 0.04	19 ± 2	100 ± 1	97.48 ± 0.09	97.50 ± 0.06	100 ± 1

Table S7. Flow cytometry data measuring the level of apoptosis in A2780 cells exposed to compound **1** at 150 nM for 24 h.

Cell state	% population ± SD	
	Compound **1**	Negative control
Alive (L)	93.1 ± 0.8	99.5 ± 0.8
Early apoptosis (A)	0.6 ± 0.2	0.19 ± 0.05
Dead (D)	5.92 ± 0.09	0.052 ± 0.006

Table S8. Selectivity data for compound **1** versus cisplatin for activity in A2780 cells and MRC-5 fibroblast cells.

	IC_{50} ± SD (μM)		Selectivity
	A2780	MRC-5	
Compound **1**	0.14 ± 0.01	4.55 ± 0.06	33X
CDDP	1.2 ± 0.1	13.4 ± 0.3	11X

Figures

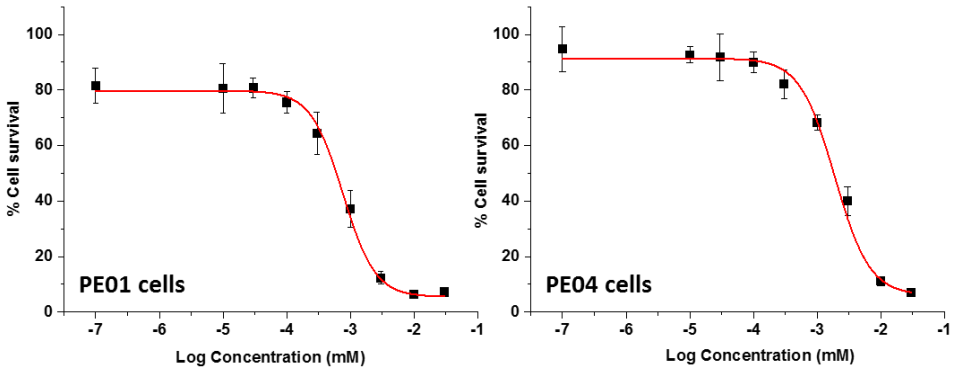

Fig. S1. Antiproliferative activity of compound **1** in patient-derived ovarian cancer cells PE01 (0.85 μM) and PE04 (2.14 μM). The PEO1 cisplatin-sensitive cell line is a BRCA2 mutant, whereas the PEO4 cisplatin-insensitive cell line exhibits a functional restoration of BRCA2 through secondary mutation (8). Thus this matched pair of patient-derived ovarian cancer cells recapitulates a clinically important acquired resistance mechanism of platinum therapy.

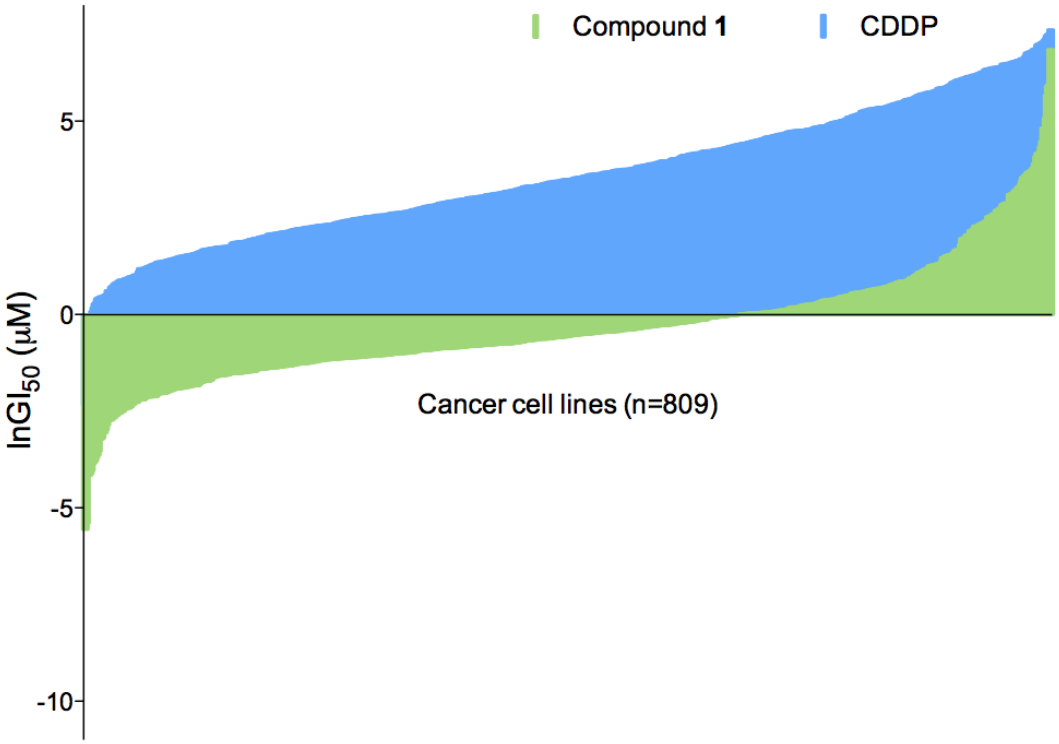

Fig. S2. Anti-proliferative activity of compound **1** (green) and cisplatin (CDDP) (blue) in 809 cancer cell lines, screened by the Sanger Institute in the Cancer Genome Project (https://www.sanger.ac.uk/research/projects/cancergenome/). The mean GI_{50} value for compound **1** is 0.75 µM and for CDDP is 36.7 µM.

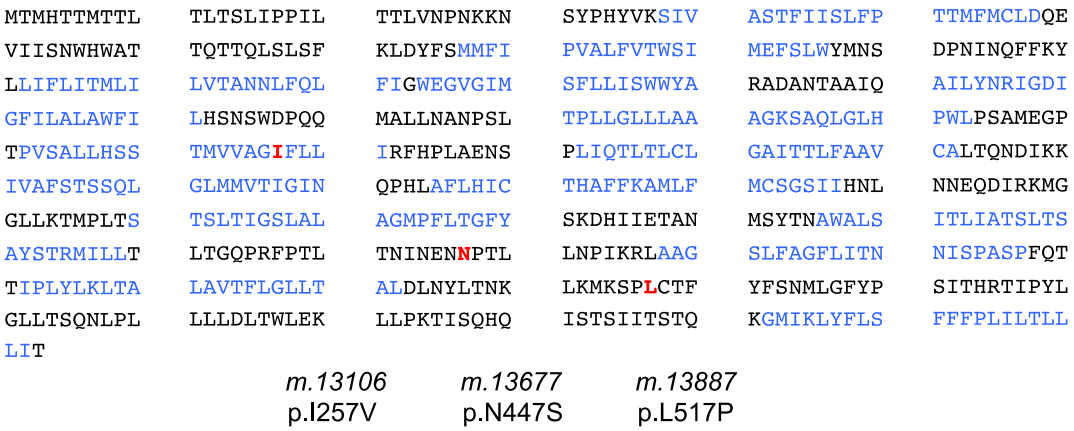

Fig. S3. Sequence of *MT-ND5* gene in the hg19 genome. Point mutations in the MT-ND5 amino acid sequence are in red; residues highlighted in blue are transmembrane α-helices in the subunit. In addition to multiple transmembrane domains, the ND5 subunit has a transverse helix, which stretches across ND4 and ND2 before ending with a final transmembrane helix (9). Only the p.I257V substitution is found in a transmembrane domain, the p.N447S substitution, known to cause CI deficiencies, is outside the membrane, and the new p.L517P substitution is found in the transverse helix.

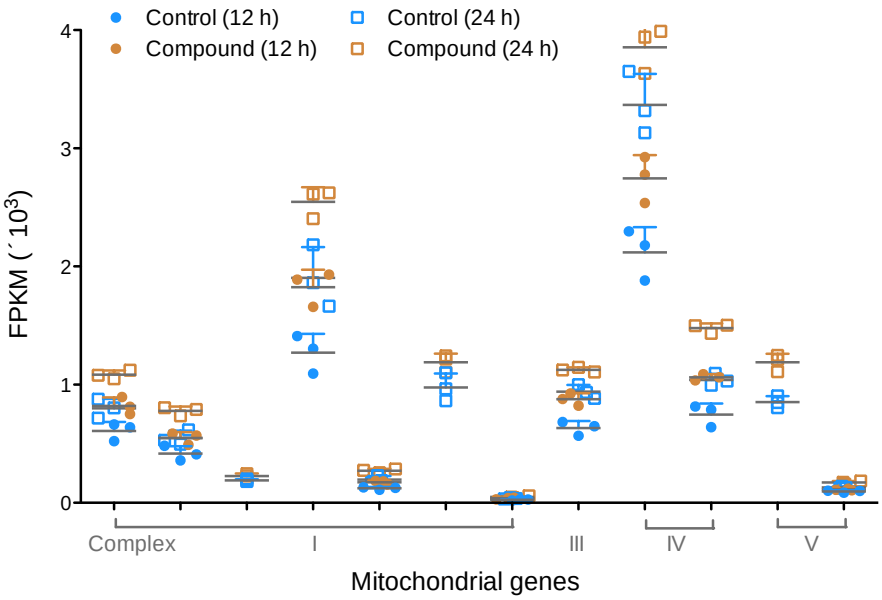

Fig. S4. Chart showing the FPKM for individual genes on the ChrM. Grey line = mean. Genes are grouped into their functional locations in the electron transport chain. Figure shows the number of normalized reads mapped to ETC-related genes, separated by their position in the pathway (complexes I-V) (10). For all ETC components, the genes with particularly high read counts encode polypeptides in the ND4 subunit of complex I (NADH dehydrogenase), and CO2 subunit of complex IV (cytochrome c oxidase). Complex I is the biggest of all the OXPHOS components, with 45 subunits, 7 encoded by ChrM (ND1, ND2, ND3, ND4, ND5, ND6, ND4L). CI is the first complex in the OXPHOS pathway and catalyzes the two-electron oxidation of NADH. The increased expression of *MT-CO2* within complex IV (CIV), Fig. 1C, may be activated in response to reactive oxygen species (ROS), due to its antioxidant effects (11). It could also relate to cytochrome c release, which constitutes an important step in apoptosis (12). Cytochrome c release is often associated with disruptions in mitochondrial membrane polarization, as we have previously shown for compound **1** (13). The up-regulation in OXPHOS components suggests that the cell utilizes this energy production pathway in response to compound **1**.

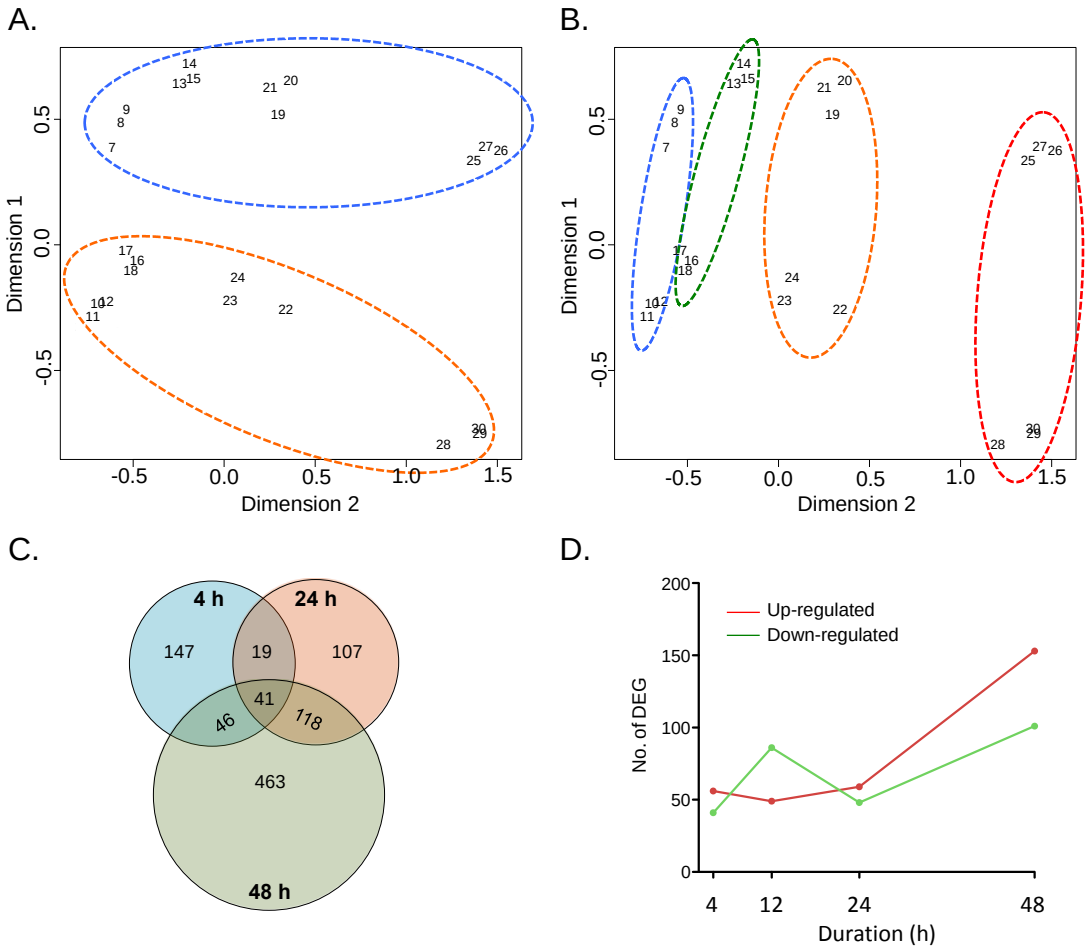

Fig. S5. The up- and down-regulation of genes in response to compound **1**. (A) Multidimensional scaling plot showing the similarity of all samples by the distance between data points. The plot highlights the separation of compound- (orange) and control-exposed (blue) samples in the 1st dimension. (B) Similarity matrix of all samples showing the separation by time series (4 h blue, 12 h green, 24 h orange, and 48 h red) in the 2nd dimension. (C) Venn diagram showing the number of DEGs with -1.5 < LogFC > 1.5 and FDR < 0.05, after 4, 24 and 48 h exposure. (D) Graph showing the number of up- and down-regulated DEGs after 4, 12, 24 and 48 h exposure.

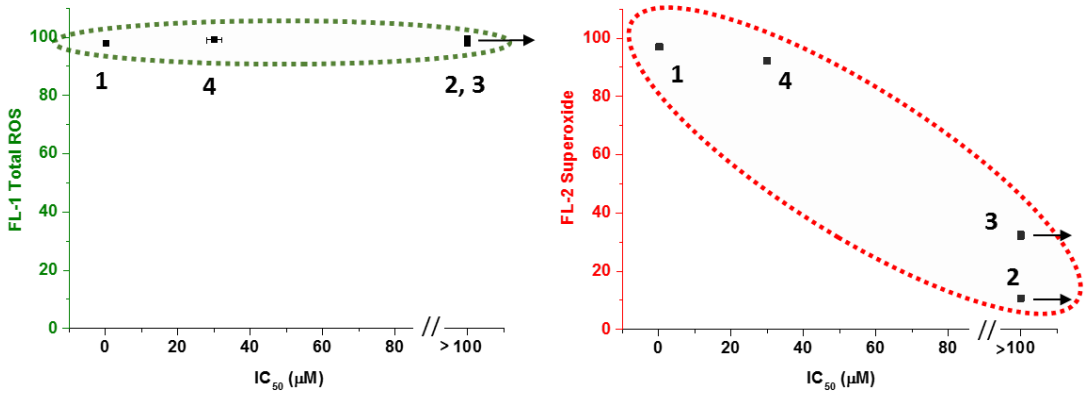

Fig. S6. Comparison of the flow cytometry analysis of ROS (left) and superoxide (right) induction in A2780 ovarian cancer cells exposed for 24 h to compounds **1-4**. The FL1 green channel detected total ROS, including peroxides, peroxynitrites and hydroxyl radicals, and the FL2 red channel superoxide levels. There is a correlation for each cell line between the antiproliferative activity (IC_{50}) of the Os(II) compound and the level of superoxide induction (**1** ([Os(η^6-*p*-cym)(NMe_2-azpy)I]PF_6, IC_{50}=0.15 ± 0.01 μM); **2** ([Os(η^6-*p*-cym)(azpy)Cl]PF_6, IC_{50} >100 μM); **3** ([Os(η^6-bip)(Cl-azpy)Cl]PF_6, IC_{50} >100 μM); **4** ([Os(η^6-*p*-cym)(OH-impy)I]PF_6, IC_{50}= 30 ± 2 μM).

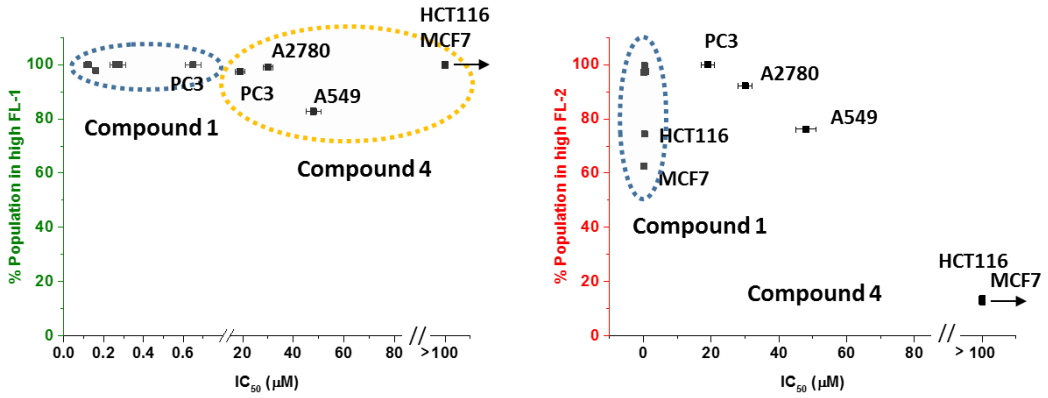

Fig. S7. Comparison of the flow cytometry analysis of ROS (left) and superoxide (right) induction in A2780 ovarian, A549 lung, HCT116 colon, MCF7 breast and PC3 prostate cancer cells caused by exposure for 24 h to compounds **1** (0.15 μM) or **4** (15 μM) . The FL1 green channel detected total ROS, including peroxides, peroxynitrites and hydroxyl radicals, and the FL2 red channel superoxide levels. There is a correlation between the antiproliferative activity (IC_{50}) of the Os(II) compounds in each cell line and the level of superoxide induction.

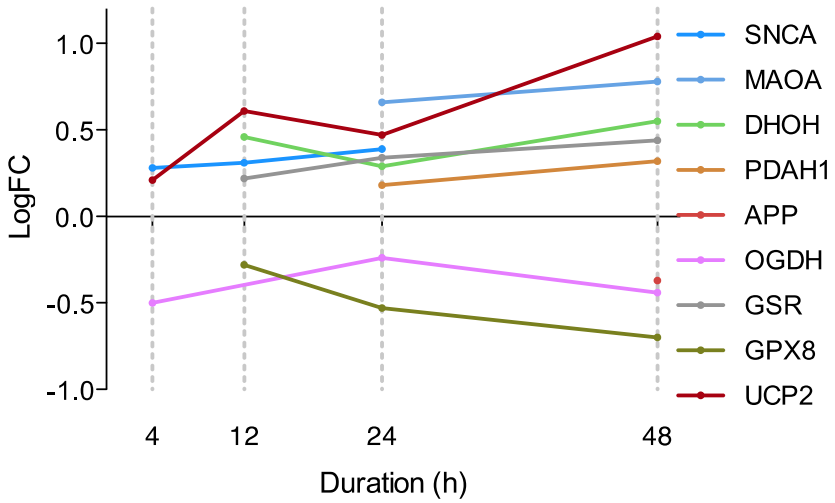

Fig. S8. Mitochondrial dysfunction in A2780 cells. Graph showing the differential gene expression, as log fold-change (LogFC), of elements involved in the mitochondrial OXPHOS pathway across the time series (FDR < 0.10).

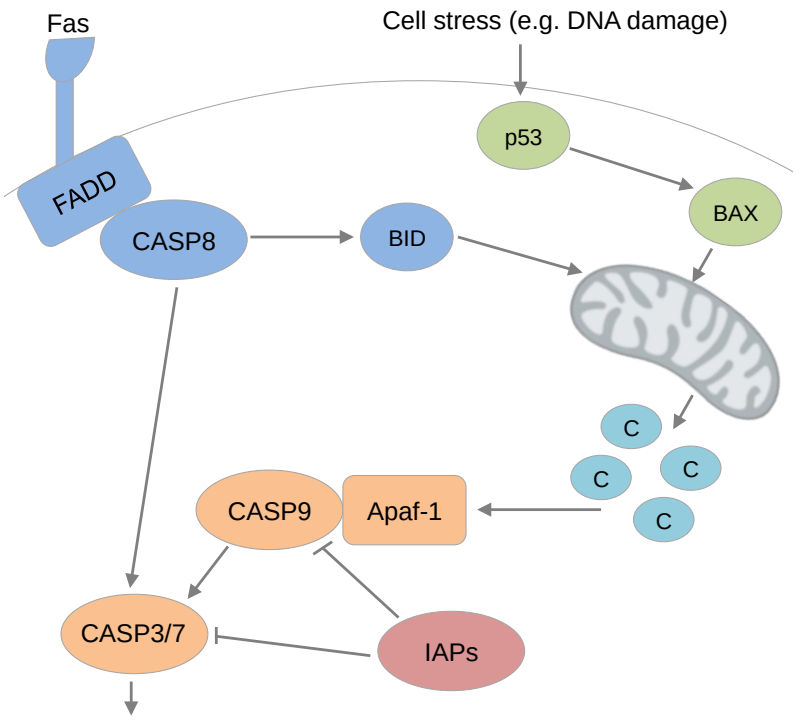

Fig. S9. Summary apoptotic network diagram. Extrinsic signals (Fas) and intrinsic signals (cell stress) resulting in caspase-3/7 activation from which apoptosis is activated.

References

1. Fu Y, *et al.* (2010) Organometallic osmium arene complexes with potent cancer cell cytotoxicity. *J Med Chem* 53:8192–8196.

2. Fu Y, *et al*. (2011) Structure–activity relationships for organometallic osmium arene phenylazopyridine complexes with potent anticancer activity. *Dalton Trans* 40:10553–10562.

3. Fu Y, *et al.* (2012) The contrasting chemical reactivity of potent isoelectronic iminopyridine and azopyridine osmium(II) arene anticancer complexes. *Chem Sci* 3(8):2485–2493.

4. Skehan P, *et al.* (1990) New colorimetric cytotoxicity assay for anticancer-drug screening. *J Natl Cancer Inst* 82(13):1107–1112.

5. Vichai V, Kirtikara K (2006) Sulforhodamine B colorimetric assay for cytotoxicity screening. *Nat Protoc* 1(3):1112–1116.

6. Langdon SP, *et al.* (1988) Characterization and properties of nine human ovarian adenocarcinoma cell lines. *Cancer Res* 48(21):6166–6172.

7. Mosmann T (1983) Rapid colorimetric assay for cellular growth and survival: application to proliferation and cytotoxicity assays. *J Immunol Methods* 64:55–63.

8. Sakai W, *et al.* (2009) Secondary mutations as a mechanism of cisplatin resistance in BRCA2-mutated cancers. *Nature* 451(7182):1116–1120.

9. Hirst J (2013) Mitochondrial complex I. *Annu Rev Biochem* 82:551–75.

10. Rich PR, Maréchal A (2010) The mitochondrial respiratory chain. *Essays Biochem* 47:1–23.

11. Taylor RW, Turnbull DM (2005) Mitochondrial DNA mutations in human disease. *Nat Rev Genet* 6:389–402.

12. Wang C, Youle RJ (2009) The role of mitochondria in apoptosis. *Annu Rev Genet* 43:95–118.

13. Van Rijt SH, Romero-Canelón I, Fu Y, Shnyder SD, Sadler PJ (2014) Potent organometallic osmium compounds induce mitochondria-mediated apoptosis and S-phase cell cycle arrest in A549 non-small cell lung cancer cells. *Metallomics* 6(5):1014–1022.